Doping and temperature dependence of Raman scattering from $NdFeAsO_{1-x}F_x$ ($x=0-0.2$) superconductor

L. Zhang,[1] T. Fujita,[1] F. Chen,[2] D. L. Feng,[2] S. Maekawa,[3,4] and M. W. Chen[1,3,*]
[1]*World Premier International (WPI) Research Center, Advanced Institute for Materials Research, Tohoku University, Sendai 980-8577, Japan*
[2]*Department of Physics, Fudan University, Shanghai 200433, China*
[3]*Institute for Materials Research, Tohoku University, Sendai 980-8577, Japan*
[4]*CREST Japan Science Technology Agency, Tokyo 102-0075, Japan*
(Received 8 September 2008; published 26 February 2009)

Raman spectra of superconductor $NdFeAsO_{1-x}F_x$ ($x=0.0,0.1,0.2$) compounds have been systematically investigated as functions of temperature and fluorine concentration. It was found that fluorine doping leads to structure disorder of insulator Nd-O layers and detectable downshift as well as increased temperature coefficients of the Fe-As vibrational modes. Additionally, low-temperature Raman measurements reveal that the in-plane phonon modes of the layered compound are unusually more sensitive to temperature change than those along the axis, and this anisotropic temperature dependence of phonon models is further enhanced by fluorine doping.

DOI: 10.1103/PhysRevB.79.052507 PACS number(s): 74.72.−h, 78.30.−j, 63.20.D−

The recent discovery of $RFeAsO_{1-x}F_x$ (R=rare-earth elements) superconductors has stimulated tremendous research interests since they are the first example of a noncuprate transition-metal compound with unconventional superconductivity and high transition temperatures.[1–8] According to traditional Bardeen-Cooper-Schrieffer theory, electrons form Cooper pairs through an interaction mediated by vibrations of crystal lattices. Thus, although superconductivity is an electronic phenomenon, it is more or less associated with the vibrations (phonons) of crystal lattices in which the electrons travel. Even though the underlying micromechanism of high-T_c superconductivity of the materials appears much more complex than that described by the traditional phonon-mediated Cooper pairs, Raman spectroscopy can still offer unique insights into the superconductivity by detecting phonons or other excitations in the superconductor compounds. Moreover, Raman spectroscopy is also a powerful tool in identifying various phases in polycrystalline inorganic materials and in studying underlying atomic and electronic structure changes caused by minor doping. In this study, we systematically investigated the microstructure and phonon modes of polycrystalline $NdFeAsO_{1-x}F_x$ ($x=0.0,0.1,0.2$) compounds at room and low temperatures and found that fluorine doping results in visible variations in atomic structure and phonon excitations of the Fe-based superconductors.

Polycrystalline samples with nominal compositions of $NdFeAsO_{1-x}F_x$ ($x=0.0,0.1,0.2$) were synthesized by a standard two-step solid-state reaction using NdAs, NdF_3, FeAs, Fe, and Fe_2O_3 (purity $>99.9\%$) as green powders. The samples with the stoichiometric ratio of $NdFeAsO_{1-x}F_x$ (14:1:1:6:4 for $x=0.2$; 29:1:1:11:18 for $x=0.1$) were sintered at 1150 °C for 48 h. Resistivity measurements demonstrate that two fluorine-doped samples, $NdFeAsO_{0.9}F_{0.1}$ and $NdFeAsO_{0.8}F_{0.2}$, are superconductors with T_c of about 33 and 51 K, respectively. The sample surfaces were carefully polished for scanning electron microscope (SEM) characterization and for Raman-scattering measurements. Crystalline phases in the sintered samples were characterized by an x-ray diffraction (XRD) spectrometer with Cu $K\alpha$ radiation ($\lambda=1.5406$ Å). Microstructure of the polycrystalline samples was inspected by SEM (JOEL JSM-7000F) and an optical microscope. Raman studies were performed by using a Raman microscope (Renishaw InVia RM 1000) with an incident wavelength of 514.5 and 632.8 nm. To avoid possible sample damage caused by laser irradiation, the actual laser power densities are set at a low value of $\sim 2.4\times10^3$ W/cm^2 for regular Raman measurements with a short-distance lens and $\sim 1.2\times10^3$ W/cm^2 for low-temperature measurements with a long-distance lens. Low-temperature Raman study was conducted using a heating/cooling stage where liquid nitrogen was used as a cryogenic source and a resistance heater for heating.[9] The sample temperatures were measured using a Pt-based thermal couple with an accuracy of ± 0.1 K.

XRD patterns of three $NdFeAsO_{1-x}F_x$ samples are illustrated in Fig. 1. Most of the diffraction peaks in the XRD spectra can be assigned to a tetragonal ZrCuSiAs-type ($P4/nmm$) phase, except for some weak peaks from second-

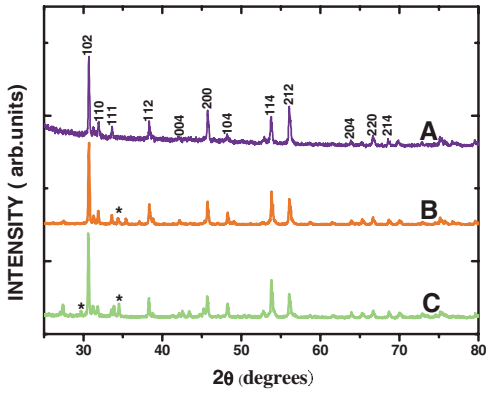

FIG. 1. (Color online) XRD patterns of polycrystalline $NdFeAsO_{1-x}F_x$ with (A) $x=0$, (B) $x=0.1$, and (C) $x=0.2$. The stars denote the peaks from the secondary FeAs phase.

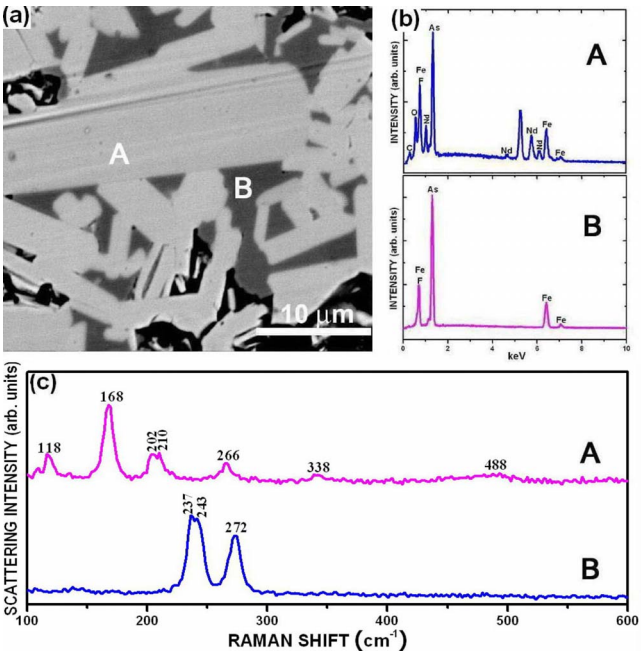

FIG. 2. (Color online) (a) Backscattering SEM micrograph of $NdFeAsO_{0.9}F_{0.1}$; [(b) and (c)] EDS and Raman spectra corresponding to (A) superconducting $NdFeAsO_{0.9}F_{0.1}$ compound and (B) the FeAs phase.

ary impurity phases.[1,7] Slight peak shift caused by fluorine doping, corresponding to the lattice-constant changes, can be detected. Moreover, the XRD spectra indicate that the fluorine-doped samples appear to contain more secondary phases. Backscattering SEM micrographs reveal that there are mainly two phases with different contrast in the polycrystalline samples. Figure 2(a) shows an example of the microstructure of the $NdFeAsO_{0.9}F_{0.1}$ sample in which chemical compositions of individual phases are measured by SEM energy dispersive x-ray spectroscopy (EDS). The white phase contains all the nominal components of Nd, Fe, As, F, and O, and thus it is the NdFeAsOF superconductor. In contrast, the dark phase is only composed of Fe and As. Combining with XRD and electron diffraction (not shown here), the secondary phase is determined to be a FeAs phase with a MnP-type crystal structure.

With the known microstructure of the polycrystalline samples, Raman spectra of the two phases were measured from the polished samples using the Raman microscope. The laser beam size used in this study is about 2 μm, which is much smaller than the grain sizes of the $NdFeAsO_{1-x}F_x$ superconductor and the FeAs phase. Thus, single phase spectra can be acquired from the polycrystalline samples in our study. Figure 2(c) shows an example of the Raman spectra of the $NdFeAsO_{0.9}F_{0.1}$ sample. It can be found that the superconductor compound that is comprised of a number of bands at about 118, 135, 168, 202, 210, 266, 338, and 488 cm^{-1} [Fig. 2(c), line a]. According to the literature, 168, 202, 210, and 338 cm^{-1} come from translational modes of the component atoms along an axis direction (the direction perpendicular to layers),[10–14] 118, 135, 266, and 488 cm^{-1} from the in-plane translational mode of Nd, As, Fe, and O, respectively.[10,11,15,16] These bands and their assignments

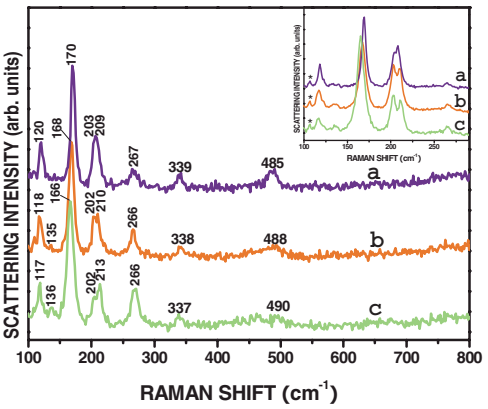

FIG. 3. (Color online) Micro-Raman spectra of $NdFeAsO_{1-x}F_x$ compounds with an incident length of 514.5 nm. (a) NdFeAsO, (b) $NdFeAsO_{0.9}F_{0.1}$, and (c) $NdFeAsO_{0.8}F_{0.2}$. The small spectra pattern shows the phonon modes at low frequencies which were measured with excitation wavelength of 632.8 nm, and the stars denote the peaks from the air.

match well with the known atomic structure of the $NdFeAsO_{1-x}F_x$ superconductor. For the secondary FeAs phase, there are three characteristic vibrational modes [Fig. 2(c), line b] at 237, 243, and 272 cm^{-1}, associated with the mixed stretching and librational vibrations of Fe-As bond.[17] It is worth emphasizing that the Raman scattering of the FeAs phase is much stronger than that of the superconductor phase, which easily causes confusion when one does not have the preknowledge of the microstructure of the polycrystalline materials.

It has been known that fluorine doping is the key leading to the metal-to-superconductor transition in the *R*FeAsO compounds at high temperatures. Thus, detecting the doping effect on atomic structure and phonon excitations may offer useful insights on the superconductivity of the Fe-based materials. Figure 3 shows the Raman spectra of $NdFeAsO_{1-x}F_x$ (x=0.0, 0.1, 0.2). The band positions and assignments of optical phonons are summarized in Table I. Visible band shift and intensity changes of the characteristic peaks of the superconductor phase can be detected with fluorine/oxygen ratios. The most notable variation caused by fluorine doping is the dramatic loss in the intensity of the plane translational mode of oxygen atoms at ~485 cm^{-1}. Meanwhile, this peak becomes broad and asymmetrical. The weakening and broadening of the oxygen plane translational mode can be observed from all spectra taken from different superconductor grains of the doped samples, which rules out the possible effect from polarizability. Thus, it can be concluded that the distribution of fluorine in the Nd-O layers is random and disorder, and the fluorine doping causes the symmetry decrease and structure disorder of insulated Nd-O layers. Additionally, the frequency shift of the characteristic Raman bands can be observed with fluorine doping. Careful measurements of the band positions demonstrate that the plane translational mode of oxygen at 485 cm^{-1} upshifts to 490 cm^{-1} with ~5 at. % fluorine doping, suggesting that the binding energy between Nd and O increases with the substitution of oxygen by fluorine. Although the structure changes mainly take place in the oxide layers, fluorine dop-

TABLE I. Characteristic Raman bands of $NdFeAsO_{1-x}F_x$. Note that the ***a*** and ***b*** directions are along the Fe-As layers (parallel to Nd-O layers) and ***c*** is the axial direction perpendicular to the ***a***-***b*** plane.

			Experimental Position(cm^{-1})		
Atom	Symmetry	Vibration	NdFeAsO	$NdFeAsO_{0.9}F_{0.1}$	$NdFeAsO_{0.8}F_{0.2}$
Nd	E_g	Nd translational mode in the ***a***-***b*** plane (Refs. 10 and 11)	120	118	117
As	E_g	Fe translational mode in the ***a***-***b*** plane (Refs. 10 and 11)		135	136
Nd	A_{1g}	Nd translational mode along the ***c*** axis (Refs. 10–14)	170	168	166
As	A_{1g}	As translational mode along the ***c*** axis (Refs. 10–14)	203	202	202
Fe	B_{1g}	Fe translational mode along the ***c*** axis (Refs. 10–14)	209	210	213
Fe, As	E_g	Mixed mode of Fe and As in the ***a*** or ***b*** direction (Refs. 11 and 16)	267	266	266
O	B_{1g}	O translational mode along the ***c*** direction (Refs. 12 and 13)	339	338	337
O	E_g	O translational mode in the ***a***-***b*** plane (Refs. 10, 11, and 15)	485	488	490

ing also causes discernible structure changes in the Fe-As layers. In the low-frequency range, the axial translational mode of Fe at 209 cm^{-1} (with the B_{1g} symmetry) upshifts to 213 cm^{-1} with 5 at. % fluorine doping, suggesting ~0.5 meV hardening of the Fe B_{1g} phonon. In contrast, the axial translational modes of Nd at 170 cm^{-1} (with the A_{1g} symmetry) and oxygen at 339 cm^{-1} (with the B_{1g} symmetry) downshift to 166 and 337 cm^{-1} with fluorine doping, corresponding to phonon softening of about 0.5 and 0.25 meV, respectively. In all the translational modes along the ***c*** axis, only the Fe phonon mode at 209 cm^{-1} shifts to higher frequency. The hardening of the Fe translational mode suggests that one main effect of fluorine doping is transferring electrons from Nd-O(F) layers to the Fe-As layers[18] and the interaction between Fe atoms increases because of the additional electrons in Fe-As layers.

Since superconducting transition occurs at low temperatures, temperature dependence of phonon vibrations of superconductor compounds may offer valuable clues on the mechanism of superconductivity. In this study, the Raman spectra of the $NdFeAsO_{1-x}F_x$ compound at temperatures ranging from 90 to 300 K are investigated (Fig. 4). In general, as temperatures decrease, the structure of a compound becomes more compact with the decrease in bond distance, leading to Raman bands shifting to high frequencies. The temperature-induced band shift of the $NdFeAsO_{1-x}F_x$ compound exhibits the similar trend. However, the temperature dependence of the Raman scattering of the $NdFeAsO_{1-x}F_x$ compound is anisotropic and the characteristic modes have different temperature coefficients. As shown in Fig. 5, in the parent NdFeAsO compound all the phonon modes show linear changes with temperatures decreasing, except the translational mode of Fe. The Fe translational mode along the axial direction at ~209 cm^{-1} shows anharmonic behavior in all the three materials[10] and the changes can be fitted with a straight line only between 298 and 150 K. The temperature coefficient of the Fe-As mode at ~266 cm^{-1} is about $(2.12 \pm 0.07) \times 10^{-2}$, which is about two times larger than that of the oxygen axial translational mode at ~339 cm^{-1} $[(1.10 \pm 0.11) \times 10^{-2}]$ and the Nd axial translational mode at ~170 cm^{-1} $[(1.32 \pm 0.18) \times 10^{-2}]$, and considerably larger than the oxygen in-plane translational mode at ~485 cm^{-1} $[(1.59 \pm 0.14) \times 10^{-2}]$. Thus, the conducting Fe-As layers are more sensitive to temperature changes than the insulator oxide layers, which is in agreement with the fact that metals generally have higher temperature coefficients than insulator ceramics. Additionally, fluorine doping enlarges the differ-

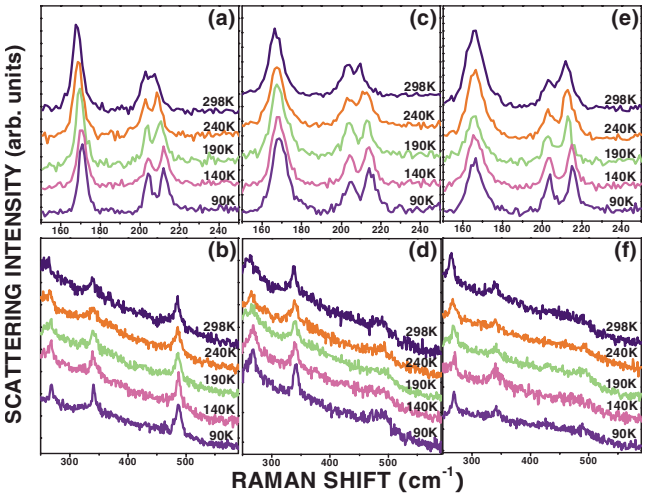

FIG. 4. (Color online) Raman spectra of $NdFeAsO_{1-x}F_x$ at the temperature ranging from 298 to 90 K. [(a) and (b)] NdFeAsO, [(c) and (d)] $NdFeAsO_{0.9}F_{0.1}$, and [(e) and (f)] $NdFeAsO_{0.8}F_{0.2}$.

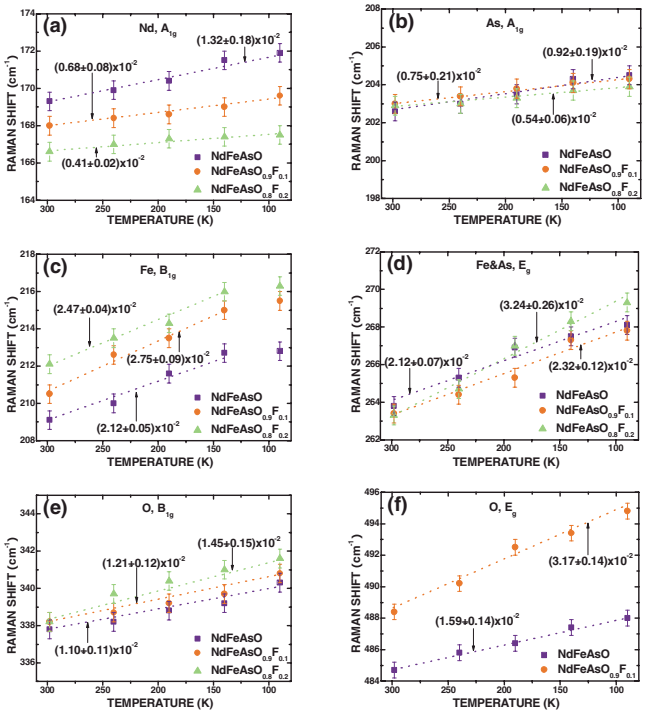

FIG. 5. (Color online) Temperature dependence of Raman bands of the superconductor $NdFeAsO_{1-x}F_x$ with various F doping. (a) Nd translational mode along the ***c*** axis, (b) As translational mode along the ***c*** axis, (c) Fe translational mode along the ***c*** axis, (d) mixed mode of Fe and As in the ***a*** or ***b*** direction, (e) O translational mode along the ***c*** direction, and (f) O translational mode in the ***a***-***b*** plane.

ence in the temperature coefficients of the characteristic modes of the superconductor compound. As we discussed before (Fig. 3), the changes in the structures of $NdFeAsO_{1-x}F_x$ with fluorine doping are mainly associated with the structure disorder of the Nd-O insulator layers caused by the substitution of oxygen by fluorine. As a result, the temperature coefficients of the O in-plane translational mode at $\sim 485\ \mathrm{cm}^{-1}$ and the Nd axial translational mode at $\sim 170\ \mathrm{cm}^{-1}$, which are seriously influenced by Nd-O bond, are susceptible to the fluorine doping. The former one increases from $(1.59 \pm 0.14) \times 10^{-2}$ to $(3.17 \pm 0.14) \times 10^{-2}$ with 2.5 at. % fluorine doping, and the latter one decreases from $(1.32 \pm 0.18) \times 10^{-2}$ to $(0.41 \pm 0.02) \times 10^{-2}$ with 5.0 at. % fluorine doping. Interestingly, the temperature coefficient of Fe-As bond at 266 cm^{-1} is also very susceptible to the fluorine doping and increases from $(2.12 \pm 0.07) \times 10^{-2}$ to $(3.24 \pm 0.26) \times 10^{-2}$ with ~ 5.0 at. % fluorine doping. The high-temperature dependence of the conducting Fe-As layers is probably related to electron-phonon interaction. It is most likely that electron doping through the replacement of O^{2-} by F^- enhances this interaction and leads to that the Fe-As layers are more metal-like, as evidenced by the increased temperature coefficient of the Fe translational mode ($\sim 209\ \mathrm{cm}^{-1}$) with fluorine doping. Comparatively, the temperature coefficients of oxygen translational modes in ***a***-***b*** plane [Fig. 5(f)] are larger than those along the axial direction [Fig. 5(e)]. The temperature coefficients of the Fe/As in-plane translational modes [Fig. 5(d)] are also larger than those along the axial direction [Fig. 5(b)]. Both of them indicate that in-plane phonon modes are more sensitive to temperature change than those along the axis in the layered compound. Moreover, this anisotropic temperature dependence of phonon models is further enhanced by fluorine doping.

In summary, we systematically investigated the Raman scattering of the polycrystalline $NdFeAsO_{1-x}F_x$ materials. With the assistance of SEM microstructure characterization, the characteristic Raman bands of the $NdFeAsO_{1-x}F_x$ superconductor were clarified. The fluorine doping was found to cause the structure disorder of the insulator Nd-O layers and thereby dramatic loss in the intensity of the oxygen in-plane translational mode. Additionally, the fluorine doping also leads to the detectable downshift and increased temperature coefficient of the Fe-As vibrational mode, demonstrating that the electron doping with F^- substituting O^{2-} results in the weakening of Fe-As bonding and the more metal-like behavior of the conducting Fe-As layers. Moreover, in comparison with the axial phonon modes, the in-plane phonon modes are more sensitive to temperature change and possess larger temperature coefficients, showing an anisotropic temperature dependence of phonon models of the layered compound.

This work was sponsored by "Global COE for Materials Research and Education" and "World Premier International Research Center (WPI) Initiative," the MEXT, Japan, and by CREST Japan Science Technology Agency.

*Corresponding author. mwchen@wpi-aimr.tohoku.ac.jp

[1] Y. Kamihara *et al.*, J. Am. Chem. Soc. **130**, 3296 (2008).
[2] H. Takahashi *et al.*, Nature (London) **453**, 376 (2008).
[3] C. de la Cruz *et al.*, Nature (London) **453**, 899 (2008).
[4] G. F. Chen *et al.*, Phys. Rev. Lett. **100**, 247002 (2008).
[5] X. H. Chen *et al.*, Nature (London) **453**, 761 (2008).
[6] F. Hunte *et al.*, Nature (London) **453**, 903 (2008).
[7] Y. Jia *et al.*, Appl. Phys. Lett. **93**, 032503 (2008).
[8] Z. P. Yin *et al.*, Phys. Rev. Lett. **101**, 047001 (2008).
[9] X. Q. Yan *et al.*, Appl. Phys. Lett. **88**, 131905 (2006).
[10] A. P. Litvinchuk *et al.*, Phys. Rev. B **78**, 060503(R) (2008).
[11] S. Mozaffari and M. Akhavan, Physica C **468**, 985 (2008).
[12] C. Marini *et al.*, Europhys. Lett. **84**, 67013 (2008).
[13] S. C. Zhao *et al.*, Supercond. Sci. Technol. **22**, 015017 (2009).
[14] V. G. Hadjiev *et al.*, Phys. Rev. B **77**, 220505(R) (2008).
[15] Y. Gallais *et al.*, Phys. Rev. B **78**, 132509 (2008).
[16] M. L. Tacon *et al.*, Phys. Rev. B **78**, 140505(R) (2008).
[17] H. D. Lutz and B. Müller, Phys. Chem. Miner. **18**, 265 (1991).
[18] J. Zhao *et al.*, Nature Mater. **7**, 953 (2008).